# Transport on Complex Networks: Flow, Jamming and Optimization

Bosiljka Tadić,[1, *] G. J. Rodgers,[2] and Stefan Thurner[3, †]

[1]*Department for Theoretical Physics, Jožef Stefan Institute, P.O. Box 3000, 1001 Ljubljana, Slovenia*
[2]*Department of Mathematical Sciences, Brunel University, Uxbridge, Middlesex UB8 3PH; UK*
[3]*Complex Systems Research Group, HNO, Medical University of Vienna,*
*Währinger Gürtel 18-20, A-1090 Vienna, Austria*

Many transport processes on networks depend crucially on the underlying network geometry, although the exact relationship between the structure of the network and the properties of transport processes remain elusive. In this paper we address this question by using numerical models in which both structure and dynamics are controlled systematically. We consider the traffic of information packets that include driving, searching and queuing. We present the results of extensive simulations on two classes of networks; a correlated cyclic scale-free network and an uncorrelated homogeneous weakly clustered network. By measuring different dynamical variables in the free flow regime we show how the global statistical properties of the transport are related to the temporal fluctuations at individual nodes (the traffic noise) and the links (the traffic flow). We then demonstrate that these two network classes appear as representative topologies for optimal traffic flow in the regimes of low density and high density traffic, respectively. We also determine statistical indicators of the pre-jamming regime on different network geometries and discuss the role of queuing and dynamical betweenness for the traffic congestion. The transition to the jammed traffic regime at a critical posting rate on different network topologies is studied as a phase transition with an appropriate order parameter. We also address several open theoretical problems related to the network dynamics.
PACS: 89.75.Fb, 89.20.Hh, 05.65.+b, 87.23.Ge

## 1. INTRODUCTION

### 1.1. Motivation

Networks form part of the basic model for virtually every known co-operative phenomenon, and the study of processes on networks is fundamental to a large part of the physical, biological, social, economic and engineering sciences [1]. Most technological, biological, economical or social networks support a number of transport processes, such as the traffic of information packets [2, 3, 4, 5, 6, 7, 8, 9, 10, 11, 12, 13, 14], signals, molecules [15], finance and wealth [16, 17, 18], rumours [19] or diseases [20, 21]. One can model these processes in many different ways, from simple interacting random walkers [22, 23, 24], to interacting random walks with random traps [25] on the network that serve as destinations, to richer models in which the traps are walker specific. Some of the models we discuss here allow an even wider range of behaviour; each walker has a destination which is known and fixed at the start, potentially allowing both local and global search and navigation strategies to be introduced to improve the efficiency of the transport.

In recent years, studies of different networks have revealed that the dynamic processes crucially depend on the topology of the underlying network structure [4, 6]. However, the precise interdependencies between the functional properties and the relevant structural parameters, which define network classes, remain largely unknown. In naturally evolved networks, such as the cytosceleton in cells, which serve as a backbone of molecular transport within the cell, efficient functioning emerges through an optimisation of function via the evolutionary adjustment of the structure. This structure–function optimization is an imperative in artificial networks because of the need for increased efficiency [26, 27], low risk of information loss, low levels of congestion [10, 28] and low risk of critical malfunction [29, 30, 31]. Therefore, understanding a network's functional properties and their dependence on a *reduced* set of its structural parameters is of paramount importance. This understanding is being developed through the systematic collection of empirical data, and through the introduction, simulation and solution of new algorithms that seek to improve one or more aspects of the functional performance of the network. This work is providing the basis for a deeper theoretical understanding of transport on networks, that allows the identification of universality classes of both network topologies and transport processes.

*Electronic address: bosiljka.tadic@ijs.si
†Electronic address: thurner@univie.ac.at

## 1.2. Methodology

This paper reviews some of the work that has been carried out to progress this agenda. In our approach both the network structure and the dynamics on the network are controlled systematically within a numerical model of information traffic. In this model the posting, navigation and queuing of packets are parameterized by a set of control parameters. Then the properties of the traffic are determined for different underlying network structures. Two approaches are available to optimise traffic. When the network structure is fixed on the time scale of the transport, one can find sets of optimal paths between nodes and specify the traffic along these paths. Alternatively, when the network structure is allowed to evolve on the same time scale as the transport, an optimal network structure is found that depends on the traffic conditions.

## 1.3. Properties of Information Traffic

The traffic of information packets is defined via several properties and parameters. Here we summarize these properties, which are later realized in the simulations.

- *Creation & Assignment.* An information packet is created, at some rate, at a node $i$ and is assigned the address of another node $j$ where it should be delivered; When a packet arrives at its destination it is removed from the network;

- *Traffic Queues.* Packets form queues when two or more packets are at same node at the same time; The queue length at node $i$ at time $t$ is denoted by $Q_i(t)$;

- *Queuing Discipline.* This determines the order in which packets leave a queue; In this work we use the last-in-first-out (LIFO) queuing discipline for traffic simulations;

- *Waiting Time $t_w$.* Is the time that a packet spends in a particular queue waiting to leave;

- *Travel Time $T$.* Is the total time that a packet spends in the network from its creation to its delivery at its destination. This time is equal to the summation of the path length and the waiting time at each queue along the path; The travel time of a packet is related to its *travel costs*, sometimes called the *search costs*.

- *Navigation & Search Depth.* Information about a packet's destination is required if one wishes to reduce its travel time by using a navigation process; Global navigation is a costly procedure in which a shortest (or the best) path for each packet is determined; A much less costly alternative is to use *local search* algorithms in which each packet explores the neighbourhood of its current node for its destination address or for an optimum direction; A search depth of $d = 1$ corresponds to the nearest-neighbourhood of a node and $d = 2$ corresponds to the next-nearest-neighbourhood a node, sometimes called *nnn*-search; A search depth of $d = 0$ corresponds to random processing; In this paper we employ $d = 2$, *nnn*-search;

- *Dynamic Load.* The number of packets transported by a node $i$, or along a link $ij$, at time $t$ defines the dynamic load of the node $h_i(t)$ and the link $f_{ij}(t)$; The total number of packets in the network $N_p(t)$ is the network load, obviously $N_p(t) = \sum_i Q_i(t)$, the sum of all queue lengths at time $t$;

- *Traffic Noise.* The time signals of temporally fluctuating variables such as $h_i(t)$, $N_p(t)$, the number of simultaneously active nodes $n(t)$, etc. are often called traffic noise signals. In particular, the set of signals $\{h_i(t)\}$ recorded at each of $i = 1, 2, \cdots, N$ nodes simultaneously form the basis for *multi-channel noise analysis*; Analogously, *traffic flow* is the same quantity defined for links rather than nodes;

- *Free Flow Regime.* Refers to the free (uncongested) flow of packets, which is compatible with *stationarity* of the traffic noise time-series;

- *Congested Regime.* Corresponds to a partial or complete jamming in networks when packets can get stuck for an indefinite time; The network load increases steadily with time, making the time-series non-stationary.

## 1.4.  Concepts

We investigate our numerical model for information packet transport on two types of networks; a clustered scale-free network and a homogeneous network, which are, respectively, representatives of the *causal* and *homogeneous* [32] network classes. The topological properties of these networks that are relevant to transport process are discussed in detail in Section 2, along with the transport rules. We then present the results of simulations of traffic on these networks. These results consist of statistical properties of traffic collected on the global network level (such as probability distributions of packet travel times and waiting time, etc.), and local (individual nodes and links) activity during transport, sometimes called multi-channel noise and flow analysis. In Section 3 the statistical signatures of traffic jamming are discussed numerically for both network types. In addition, we consider the transition to the congested traffic phase, where travel and waiting times tend to diverge, as a dynamical phase transition. Section 4 discusses two optimization procedures, one with fixed network geometry, as above, and the other which involves the network restructuring in order to minimize the packet travel times. We show that the emergent optimized structures in low and high density traffic are statistically similar to the structures discussed in Section 2. In Section 5 we give a summary of the results and some open theoretical problems posed by the numerical simulations and by empirical measurements in real communication networks.

# 2.  STATIONARY TRAFFIC FLOW

In the first part of this section we introduce two networks—a grown scale-free correlated network, which we call the Webgraph, and a homogeneous network with a stretched-exponential degree distribution, which we call Statnet. We briefly summarise the structural properties of these networks that are relevant to their transport processes. We then introduce the model of packet transport and perform simulations on these networks with $N = 1000$ nodes. The results we obtain for the statistical properties of the transport in the *free flow* regime are presented.

## 2.1.  Structural Properties of the Networks

We consider two networks assembled by *preferential attachment* [33] and in which *rewiring* [34] occurs.

The Webgraph is grown by *sequentially adding nodes* from $i = 1, 2, \cdots N$, with linking rules that involve preferential attachment and preferential rewiring according to the time dependent probabilities $p_{in}$ and $p_{out}$. They are applied in the subset of *pre-existing* nodes at each growth step $i$. The linking probabilities depend on the current number of incoming $q_{in}$ and outgoing $q_{out}$ links at a node [34]

$$p_{in}(k,i) = \frac{\alpha + q_{in}(k,i)/M}{(1+\alpha)i} \qquad p_{out}(n,i) = \frac{\alpha + q_{out}(n,i)/M}{(1+\alpha)i} \quad . \tag{1}$$

Linking to a new node occurs with probability $\tilde{\alpha}$ and rewiring or adding a link from a previously existing node occurs with probability $1-\tilde{\alpha}$. These competing processes lead to an emergent structure [34] which is different to the structure obtained by common preferential attachment, [33, 35]. The parameters of the model $\tilde{\alpha}$, $\alpha$, and $M$ are responsible for the graph's flexibility, connectivity profile and clustering. In particular, when $\tilde{\alpha} = 1$ the graph is rigid (rewiring can not occure) and scale-free, i.e., for $M = 1$ a scale-free tree and when $M > 1$ a weakly clustered uncorrelated scale-free graph emerges as known in Refs. [33, 35]. However, when $\tilde{\alpha} < 1$, these rules lead to power-law distributions of both in-degree and out-degree [34], a large clustering coefficient and link correlations [36], even for $M = 1$. When $\tilde{\alpha} = \alpha = 1/4$ the structure is very similar to the world wide web [34]. This is why we call this network the Webgraph. An example of the emergent structure is shown in Fig. 1a.

To grow the Statnet we apply the same rules with the probabilities in Eq. (1), however, with the fixed number of nodes $i = N$, among which *links are added sequentially*. Multiple linking between the same pair of nodes is not allowed. The Statnet emergent structure, with $L = N = 1000$, is also shown in Fig. 1b.

A detailed quantitative analysis of the structure reveals that both incoming and outgoing links behave the same statistically, and exhibit a stretched-exponential degree distribution. In addition, the clustering in this graph is small compared to the Webgraph and link correlations are entirely absent. A comparison of the structural properties of both networks is given below.

*Connectivity:* The emergent connectivity of nodes in the evolving Webgraph can be obtained analytically using linking probabilities in Eqs. (1). Both for in-coming and out-going connectivity we have a power-law profile according to [37]
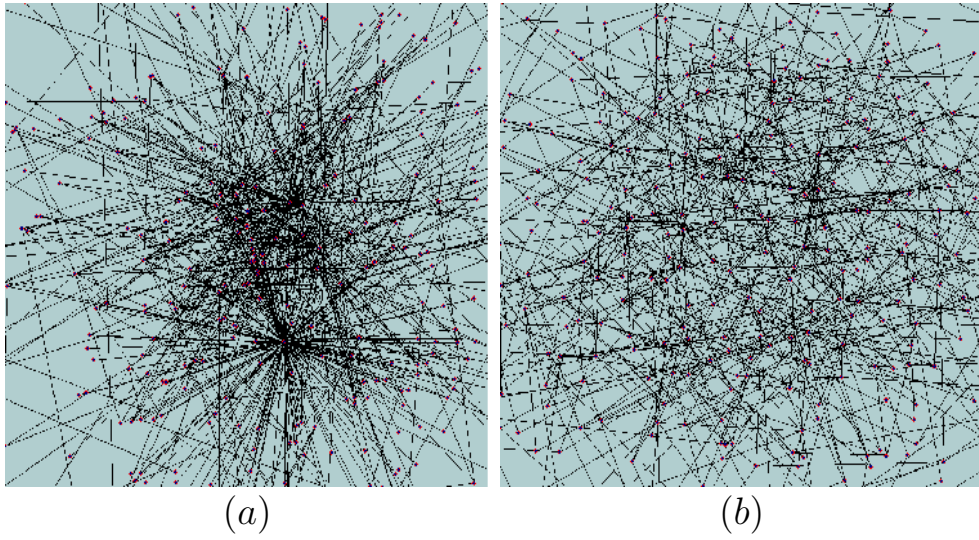
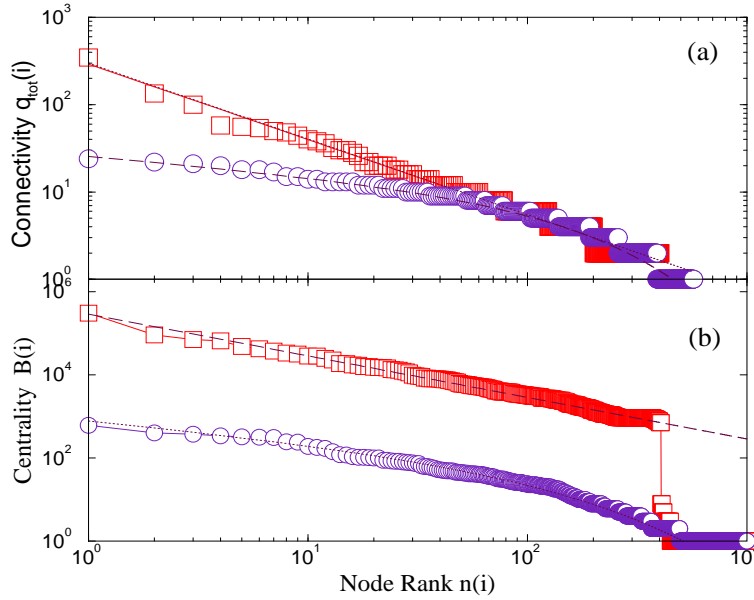FIG. 1: (a) The cyclic scale-free Webgraph and (b) homogeneous Statnet.



FIG. 2: (a) Node ranking of the total connectivity $q_{tot} = q_{in} + q_{out}$ and (b) node ranking of the topological centrality $B(i)$ in the Webgraph ($\square$) and Statnet ($\bigcirc$) structures. The fits are explained in the text.

$$q_\kappa(s, N) = A_\kappa \left[ \left( \frac{N}{s} \right)^{\gamma_\kappa} - B_\kappa \right] \; ; \tag{2}$$

after $N$ nodes are added, $s$ being the addition time. Here $\kappa$ indicates 'in', 'out', or 'total' links, for which different exponents are found [37, 38]. For the purposes of this work, we consider that the transport along a link in both directions is symmetrical. Therefore, the total node connectivity $q_{tot} \equiv q_{in} + q_{out}$ is relevant. In Fig. 2a we show the connectivity profile of all nodes in one Webgraph sample (shown in Fig. 1a). It exhibits a power-law decay with rank $n \equiv n(i)$ of a node $i$ according to

$$X(n) \sim n^{-\gamma_{tot}} \; ; \tag{3}$$

with $\gamma_{tot} = 0.867$. This indicates a power-law connectivity distribution with the exponent $\tau_{tot} = 1/\gamma_{tot} + 1 = 2.153$. Similarly, node ranking according to the total connectivity in the Statnet, also shown in Fig. 2a, is well fitted by a stretched-exponential curve

$$X(n) = An^{-\tau} \exp\left[-(n/n_0)^{\sigma}\right] ; \tag{4}$$

with $\tau \approx 0.22$, $\sigma \approx 0.78$, and $n_0 \approx 200$. The emergent probability distribution also obeys this law, Eq. (4).

*Centrality:* Further quantitative differences between these two networks are found in the node ranking using the topological centrality measure [39, 40, 41]. In Fig. 2b the ranked profile of topological betweenness of nodes are shown. For the Webgraph the profile is a power-law Eq. 3 with the exponent $\gamma_B = 1$, indicating the distribution of node betweenness as $P(B) \sim B^{-2}$. In the case of Statnet the profile is again closer to a stretched-exponential form Eq. (4). In Fig. 2b one can also identify the nodes belonging to the giant cluster, whose size is 403 nodes in the Webgraph, and 571 in the Statnet (jump).
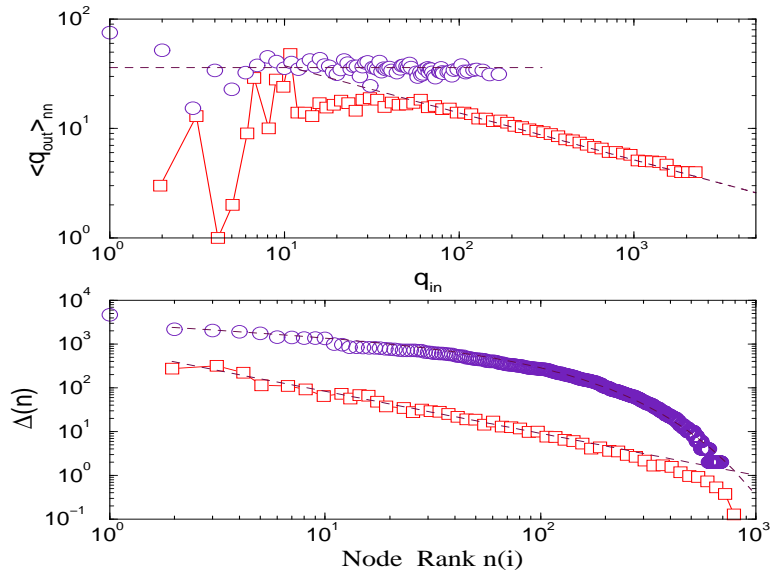


FIG. 3: Link-correlations (top) and ranked clustering profile (bottom) for the Webgraph ($\square$) with $L/N = 1$ and Statnet ($\bigcirc$) with $L/N = 20$ corresponding to the same average clustering coefficient, $cc = 0.36$.

*Clustering:* Due to the rewiring, some nodes and/or smaller clusters remain disconnected from the giant component, whereas other nodes gain large connectivity and clustering. When the average number of links per node is $M \equiv L/N = 1$ the average clustering coefficient in the Webgraph appears to be $cc = 0.3601$. In contrast Statnet, with same average connectivity $M = 1$, has a much lower average clustering $cc = 0.0075$, which increases with $M$. The clustering profile is inhomogeneous in both networks. It obeys a power-law, shown in Fig. 3a with an exponent close to $\gamma = 0.85$ in the Webgraph, where most of the elementary triangles are attached to the main hubs. In the case of Statnet a stretched-exponential profile is found.

*Correlations:* Another interesting feature which might influence the transport processes with search is found in the link correlations of the Webgraph, which are entirely absent in Statnet. The computed correlation property $\Delta_i$, denoting the number of elementary triangles attached to a node $i$, is shown in Fig. 3b for both graphs after ordering. The power-law decay with the exponent $\gamma_c = 0.42$ in the Webgraph indicates *disassortative* [42] link correlations.

## 2.2. Implementation of Constant-Density Traffic

We model the traffic of information packets on a network as a *guided random walk* between specified pairs of nodes [3, 4, 36]—the origin and destination (delivery address) of a packet. Once created, packets navigate through the network using a local *nnn*-search rule [3, 36, 43], in which the next-nearest-neighbourhood is searched for the destination node. If a node finds that a packet's destination node is in its nearest neighbourhood, it moves the packet directly to its destination. If the destination node is in the next-nearest-neighbourhood, but not the nearest-neighbourhood, the packet moves in the correct direction. If the destination node isn't found in the next-nearest-neighbourhood, the packet moves to a randomly chosen neighbouring node. Packets are removed when they arrive at

their destinations. In this section we model traffic with a *fixed number of moving packets*, which is set at the start of the simulation, so that $N_p(t) = \rho$, fixed for all $t$. Packets that arrive at their destinations and are removed from the network are replaced in the next time step by the creation of the same number of new packets at randomly chosen nodes. Of course, these packets are given new destinations. When $\rho = 1$, this corresponds to the sequential random walk problem. At density $\rho > 1$, packets interact by forming queues at nodes along their paths. We assume finite maximum queue lengths of $H = 1000$ at all nodes, and we employ a LIFO (last-in-first-out) queuing discipline.

Constant-density traffic is interesting because the limit of non-interacting packets $\rho = 1$ is mathematically correctly implemented. This enables quantitative analysis of the structure–dynamics interdependences without additional dynamic effects [43]. Also, at finite traffic density $\rho > 1$, the system is driven *self-consistently*, without external forcing. This situation is suitable for the analysis of time-series and noise fluctuations (see later), which are sensitive to driving modes. Other driving conditions, e.g., constant posting rate $R$ [3, 4, 5, 44], will be considered in Section 3 in connection with traffic jamming. When the traffic is driven by creating at each time step a number of packets which is larger than network's output rate, the network experiences congestion [6]. Driving at constant rate $R$ is appropriate for a quantitative study of the congestion problem (see Section 3).

For the numerical implementation of the transport, we first generate the network and its adjacency matrix is stored and remains fixed throughout the transport process. If the graph is disconnected, as is the case with both Webgraph and Statnet, we take care that the creation and destination nodes are within the same cluster. We study networks consisting of $N = 1000$ nodes. Starting with $\rho = 100$ packets, which are created at random positions, the network is updated in parallel. At each time step a node with a packet on it tries to move the top packet in its queue towards that packet's destination node. A packet is moved to one of node's neighbours, and joins the top of its queue. If that neighbour is the packet's destination node, the packet is considered as delivered and disappears from the network. During the transport process, for each packet we keep track of its destination, current position, and position in the current queue. In addition, for a subset of labeled, $N_M = 2000$, packets we keep track of the time that they spend in each queue before they arrive at their destination. We compute the statistical properties of the transport from the data gathered from the labeled packets once all of them have arrived at their destinations.

### 2.3. Global Transport Characteristics

The statistical properties of traffic depend on both the network structure and traffic conditions. For a fixed navigation protocol (*nnn*-search in this case), the efficiency of transport depends on the structural characteristics of the underlying network and on the overall traffic density. In particular, the travel time of packets is determined by the length of the path selected between the origin and destination node, and the waiting times at nodes along that path. That is, for a packet traveling along a path of length $k$, the travel time is given by

$$T_k = \sum_{i=1}^{k} t_w(i) \ , \tag{5}$$

where $t_w(i)$ is a packet's waiting time on node $i$ on that path. It should be stressed that both path lengths and set of waiting times $\{t_w\}$ which contribute to the travel time $T$ are outcomes of a stochastic process. Then the functional central-limit theorem [45] applies to the distribution of travel times $P(T)$, computed along all paths on the network [3]. The fact that on structured networks the waiting times along a particular path depend on the identity of nodes along that path adds to the complexity of the problem [3].

In the limit of non-interacting packets $\rho = 1$, the waiting times are $t_w = 1$ for all nodes, thus the entire travel time is determined by the geometry. The suitability of the navigation algorithm for a given topology can then be measured by the deviation of the actual path of the packet from the *shortest path* between the pair of nodes. In Fig. 4 we show how the distributions of the travel times for the Webgraph and Statnet geometries and $\rho = 100$ packets. For *nnn*−search these distributions exhibit power-law tails with different exponents on the two networks. However, the largest difference appears for short travel times, where packets follow more closely the topological shortest path on the underlying network. In this respect the node connectivity and centrality play an important role (see Fig. 2). The deviations from the shortest paths are experienced by packets which, i.e. local search being ineffective, appear to perform a random walk in parts of the graph far away from their destinations. The distributions of travel times at large density $\rho = 100$ appear to be well fitted with a power-law

$$P(T) = AT^{-\tau_T} \ ; \tag{6}$$

with $\tau_T \approx 1.5$ and an exponential cut-off (due to the finite network size) for packets on the Webgraph, and a $q$−exponential distribution

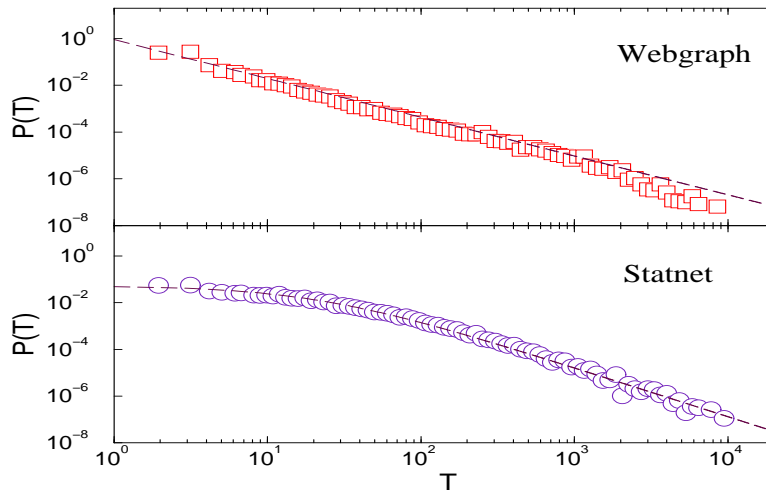$$P(T) = B_q \left[ 1 + (1-q)T/T_0 \right]^{1/(1-q)} \ ; \tag{7}$$

FIG. 4: Distribution of travel times in the Webgraph and the Statnet for a density $\rho = 100$.

with $q = 1.47$, for the case of transport on the Statnet (cf. Fig. 4).

In processes in which diffusion dominates, the topology of actual paths gives another view of the process. In particular, on structured networks, apart from the inhomogeneous connectivity, the number of short and long cycles may effect the diffusion of packets. The network profile of the short cycles (triangles) in the Webgraph and Statnet are shown in Fig. 3. The packets that perform a random diffusion, i.e. when the local search is for them ineffective, may return to a node, which had already been visited in the past. The distribution of the return-time intervals, $\Delta t_i$, for each node $i = 1, 2, \cdots N$ on the network, is given in Fig. 5 for both network types. Broad distributions with
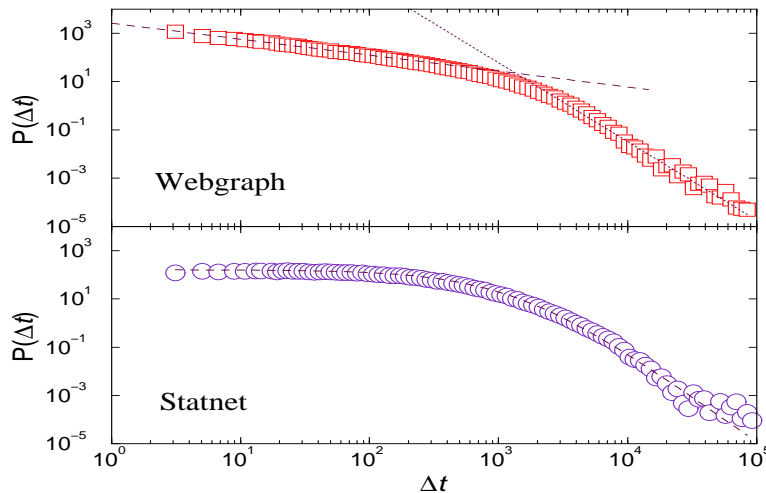


FIG. 5: Distribution of return times of packets in Webgraph and Statnet for a density $\rho = 1$.

characteristic power-law tails, suggest correlated events. Again the main difference between the two network types appears in the small return times of packets. A power-law with small slope $\tau_\Delta = 0.66$ for $\Delta t \lesssim 800$ can be related with an uneven population of short cycles and the active role of individual nodes in the case of Webgraph. In the case of Statnet the distribution can be fitted to the general expression in Eq. (7), with $q = 1.26$. On the Webgraph, the probability of long return times falls off as $P(\Delta t) \sim (\Delta t)^{-3.26}$. When the packet density is finite, the return time of node activity (where generally a different packet is involved) is different on the two networks. The distribution is shifted towards shorter values in the case of Webgraph. On Statnet the form of the distribution changes.

For large packet density $\rho >> 1$, motion of a packet will be affected by other packets moving through the same node, as mentioned above. Queues of packets then occur and a queuing discipline sets the order of processing (LIFO
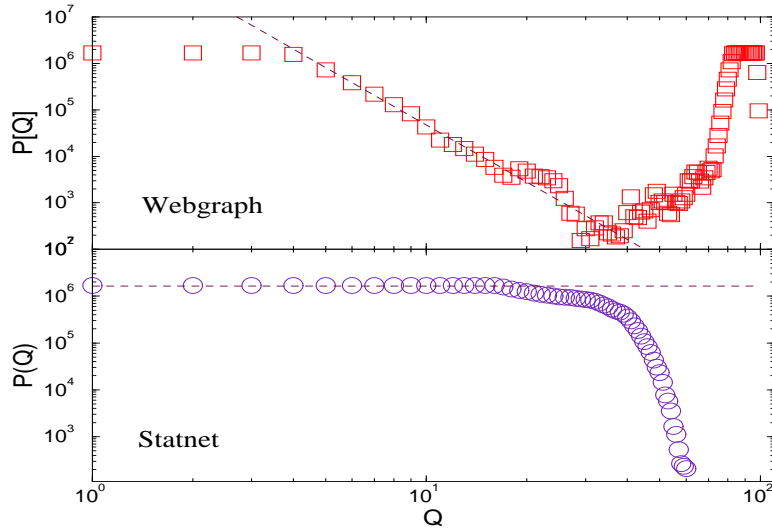
FIG. 6: Distribution of queue-lengths in Webgraph and Statnet for a packet density $\rho = 100$.

in this particular case). Apart from the traffic density, the neighbourhood of the node determines the length of the queue at that node. In particular, on inhomogeneous networks, hubs appear to receive more packets compared to other nodes, due to their large connectivity. Since in the algorithm one packet is processed per time step, other packets remain in the queue to be processed later (when no new packet has been received). The distribution of queue lengths therefore reflects the network structure in a particular way. A snapshot of queue-lengths $Q$, for traffic density $\rho = 100$ in the two network structures leads to the distributions shown in Fig. 6.

In the homogeneous Statnet most of the nodes are processing a similar number of packets, which leads to a flat distribution of queues and a cut-off indicating that queues longer than $Q \approx 40$ rarely occur. On the other hand, a large queue of $Q = 80$ to $90$, packets can be found on the hubs on the inhomogeneous Webgraph with high probability. On the rest of the nodes the queues are distributed with a power-law distribution, apart from very small queues at boundary nodes.
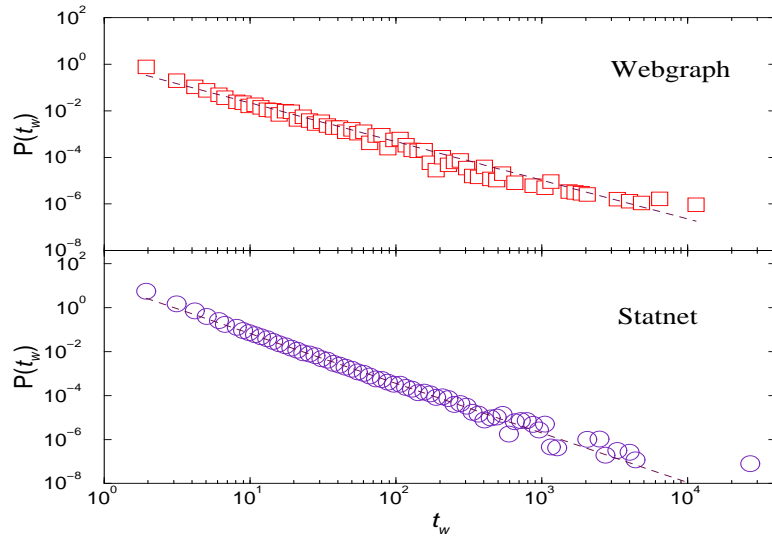


FIG. 7: Distribution of waiting times in the Webgraph and the Statnet for a density $\rho = 100$.

The queuing times of packets extend their travel times, thus reducing the overall traffic efficiency [4]. Note, that in the current implementation, with a constant number of moving packets, jamming cannot occur as long as the traffic density $\rho < H$, where $H$ is the maximum allowed queue length. However, due to long waiting times in queues, the

travel times of packets given by Eq. (5), can become very long, given by a power-law distribution, as shown in Fig. 4 (see also [3, 43] for different types of graphs and search algorithms). The distributions of waiting times of packets on two network geometries are given in Fig. 7, for the traffic density $\rho = 100$. They can be described as power-law distributions,

$$P(t_w) \sim A t_w^{-\tau_w} \; ; \tag{8}$$

with different exponents, closely related to the tails of the travel-time distributions in Fig. 4. Specifically, in the case of Statnet the numerical value of the exponent is $\tau_w \geq 2$, suggesting finite average waiting times, and thus finite travel times for packets on this network structure. In contrast, the average waiting time on the Webgraph for this traffic density is not bounded in a mathematical sense, having $\tau_w < 2$. This implies a systematic increase of the travel times of packets on a large network with this structure (with large measurement time). The distribution of waiting times and travel times of individual packets provide a quantitative measure that supports the conclusion that the Webgraph class of networks, although much more efficient compared to other scale-free network types [3, 4], is the less efficient of the two networks at high constant density of packets. More homogeneous structures, such as the Statnet, appear to perform better under these traffic conditions. It should be stressed that the waiting times as well as travel times are traffic properties measured for individual packets, which will depend on the type of queuing discipline used.

### 2.4. Noise and Flow on Networks

The observed queue lengths are compatible with the the temporal properties of node activity on the two networks, shown in Fig. 8. While queues at important nodes in the inhomogeneous Webgraph are long, the number of nodes that are simultaneously active is small, fluctuating about an average value $n_a \approx 8$. Compared to the more homogeneous Statnet for the same traffic density, on average $n_a \approx 80$ nodes are processing a packet simultaneously, leading to short queues at all nodes. Further quantitative analysis of the time-series reveals the differences in the packet processing
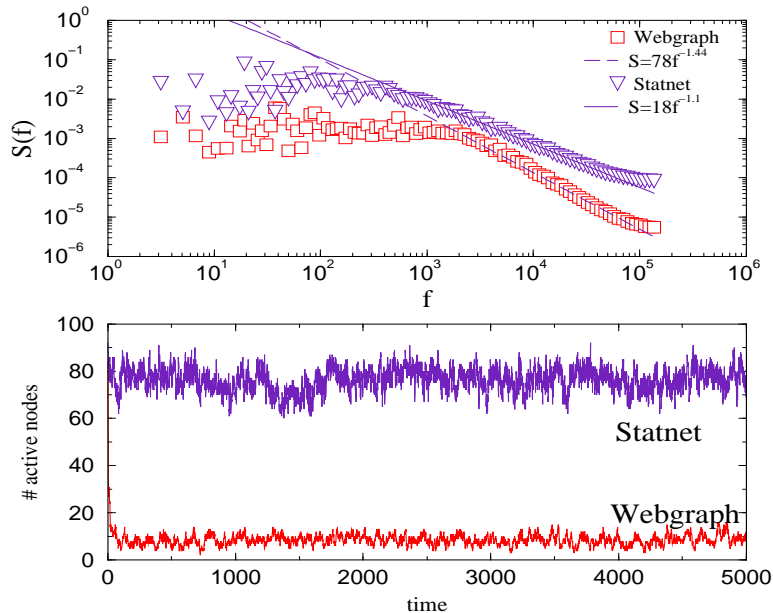


FIG. 8: Temporal fluctuations of the number of active nodes in Webgraph and Statnet (lower panel) and their power spectra (top panel) for a density of $\rho = 100$ packets (from [Tadic and Thurner, 2006]).

of the two classes of networks. In particular, long-range correlations (anti-persistence) in the number of active nodes develops on both networks. However, in the conditions of constant packet density the fluctuations on the Statnet appear to be more correlated compared to the Webgraph. The power spectrum exhibits an asymptotic power-law behavior

$$S(f) \sim f^{-\phi} \quad , \tag{9}$$
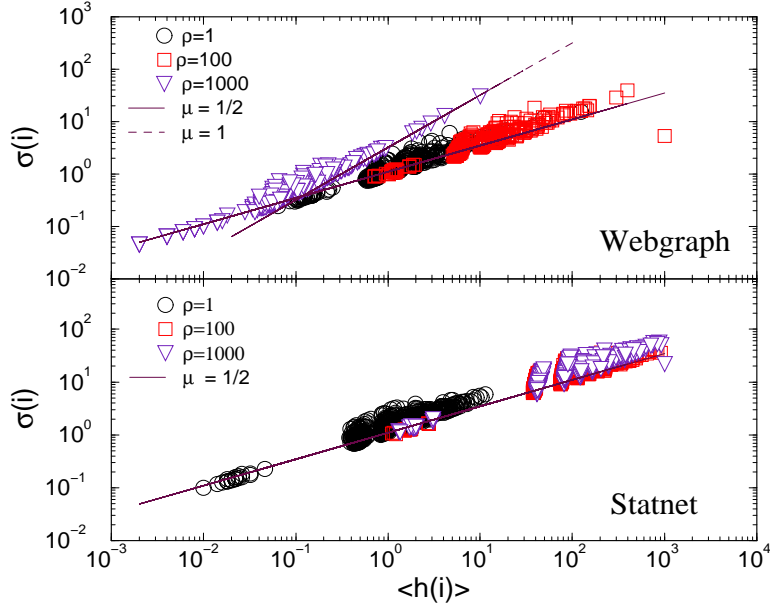
FIG. 9: Universal noise fluctuations for traffic with constant-density $\rho =$1, 100, and 1000 packets and with $nnn$-search on the for the Webgraph and Statnet. Lines indicate scaling dependences in Eq. (10), with slopes $\mu = 1/2$ and $\mu = 1$.

shown in Fig. 8 (top panel), with $\phi = 1.1$ for Statnet and $\phi = 1.4$ for the Webgraph. Therefore, an increased traffic density leads to stronger correlations in node activity on the more homogeneous Statnet [46].

The observed differences that individual nodes on each network play in the transport processes are further quantified by analysis of the noise fluctuations. We measure the number of packets $h_i(t)$ that a node $i$ processes within a fixed time window of $T_{WIN} = 1000$ time steps. We consider simultaneously (multi-channel noise analysis) a set of time-series $\{h_i(t)\}$ for all $i = 1, 2, \cdots N$ nodes and $t = 1, 2, \cdots 500$ successive time windows. We determine the standard deviation $\sigma(i)$ for each of $N$ time-series (i.e., for each node) and plot it against the time-averaged value $\langle h(i)\rangle \equiv \langle h_i(t)\rangle_t$, where the average is taken over all time windows for each node separately. The general scaling relation [47]

$$\sigma(i) \sim \langle h(i)\rangle^{\mu} , \tag{10}$$

holds for all nodes in the network for our constant-density traffic. However, we find that the scaling exponents may depend on the traffic density in the inhomogeneous Webgraph. The results are shown in Fig. 9 for the two network structures and three different traffic densities $\rho$. In particular, when the packet density is high, the number of packets processed by the hub nodes increases, resulting in the increased fluctuations at these nodes. When density is comparable with the maximum buffer size (in our case $\rho = H = 1000$), temporary congestion may occur at the main hubs and at other nodes of large connectivity, whereas the rest of the network functions in the free flow regime. In this situation, the noise fluctuations at more important nodes appear to be in the $\mu = 1$ class, as opposed to the rest of the network, where the fluctuations follow the law with $\mu = 1/2$, as shown in Fig. 9. Due to the absence of hubs in the Statnet the fluctuations remain homogeneous and in the $\mu = 1/2$ class for all packet densities.

Our results demonstrate that inhomogeneous noise fluctuations may occur in the self-regulated (constant density) traffic away from the two universality classes defined by [47]. (See also [13] for traffic self-regulation with a local feedback). In our study the explanation of these non-universal noise fluctuations is found in how the network structure handles high density traffic. These findings are in agreement with a recent detailed study of the empirical data of the Internet traffic and in a specifically designed model by [48], which revealed that when the traffic density is high "enough", then other parameters of the dynamics and structure play a role in determining the noise properties. In particular, the exponent values may vary between 0.5 and 1, depending critically on the width of the time window and on the queuing times of packets [48]. (Similar time-window effects are discovered by [49] in the stock market dynamics). Compared with earlier models which tackle the scaling of traffic noise in the Internet [7, 13, 47, 48], the traffic model that we study here is more complex in that packets are navigated to specified destinations, and that both travel times and queuing times of packets are self-consistently determined and appear to have power-law distributions (cf. Figs. 4 and 7). In the future we would hope to determine how these traffic properties contribute to the observed non-universality in noise fluctuations.

### 3.  TRAFFIC JAMMING & STRUCTURE

A crucial feature of transport networks is that they cease to function efficiently when jamming of nodes occurs. Jamming is characterized by a drastic decrease of efficiency, in particular a non-stationary increase of the load as a function of $R$. Jamming occurs as a transition at a critical rate $R_c$. It is of relevance to find alternative indicators or signatures, which are able to signal the occurrence of jamming. In particular we focus on exploring the possibility to predict the 'distance' to the jamming transition from the activity time-series of individual nodes.
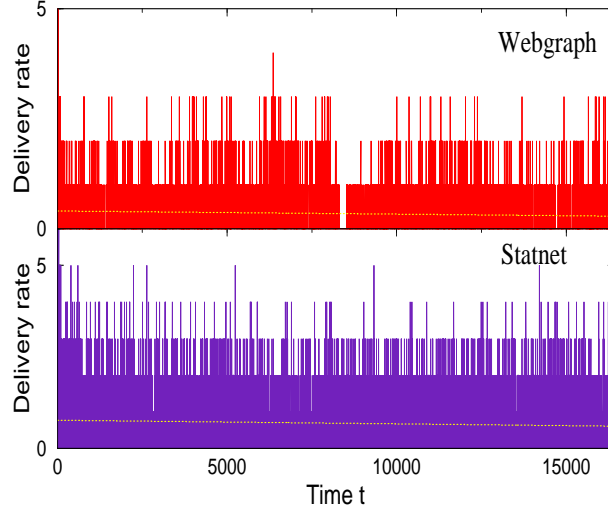


FIG. 10:  Number of packets delivered per time step $n_d(t)$ against time $t$ for fixed density of moving packets $\rho = 100$ in Webgraph and Statnet. Dotted lines indicate values of average output rate $\lambda$.

As will be discussed in Section 4, networks of different structures perform differently when the traffic density is varied. In the constant-density traffic $\rho = 100$ we show here that the network output, defined as the number of packets delivered per time step $n_d(t)$, is larger in the homogeneous Statnet compared with the scale-free Webgraph. In Fig. 10 we display the time variation of the network output $n_d(t)$ rate for the two networks. The *average output rate* $\lambda$ is defined as

$$\lambda \equiv < dn_d(t)/dt > \quad . \tag{11}$$

In the Webgraph $\lambda = 0.37$ we find packets per time step, compared with Statnet, where $\lambda = 0.71$. This difference suggests that with an imposed traffic density and a constant number of moving packets of $\rho = 100$, the traffic on the Webgraph topology is closer to jamming than the Statnet topology. In this Section we will explore in more detail the statistical signature of traffic near jamming.

### 3.1.  Queuing and Jamming at Different Topologies

The approach to the jamming regime is most appropriately studied with a *constant posting rate $R$*. Then the temporal variations in the network load $N_p(t)$ are given by

$$N_p(t) = Rt - n_d(t) . \tag{12}$$

When the posting rate $R$ increases so that it exceeds the average output rate, $R > \lambda$, the excess packets accumulate on the network leading to a systematic increase in the network load $N_p(t)$, although the network continues to deliver packets in some way. The average accumulation rate is then obtained from Eq. (12) as

$$J \equiv < dN_p(t)/dt >= R - \lambda \quad , \tag{13}$$

which is reminiscent of the congestion condition $J/R = 1 - \lambda/R$, often found in queuing theory for a single-server queue [45, 50]. It should be stressed, however, that here the load $N_p(t)$ applies to the whole network, which consists of many interacting queues. The excess load increases the queues at different nodes, depending on each node's topological

centrality and its importance in the particular transport process. Therefore, subtle interactions between different queues and their dynamical correlations contribute to the jamming process, which are different for different network topologies. This aspect of network congestion will be discussed in detail later. We first demonstrate how the statistical properties of the traffic change with increased posting rate by simulating traffic on the Webgraph.
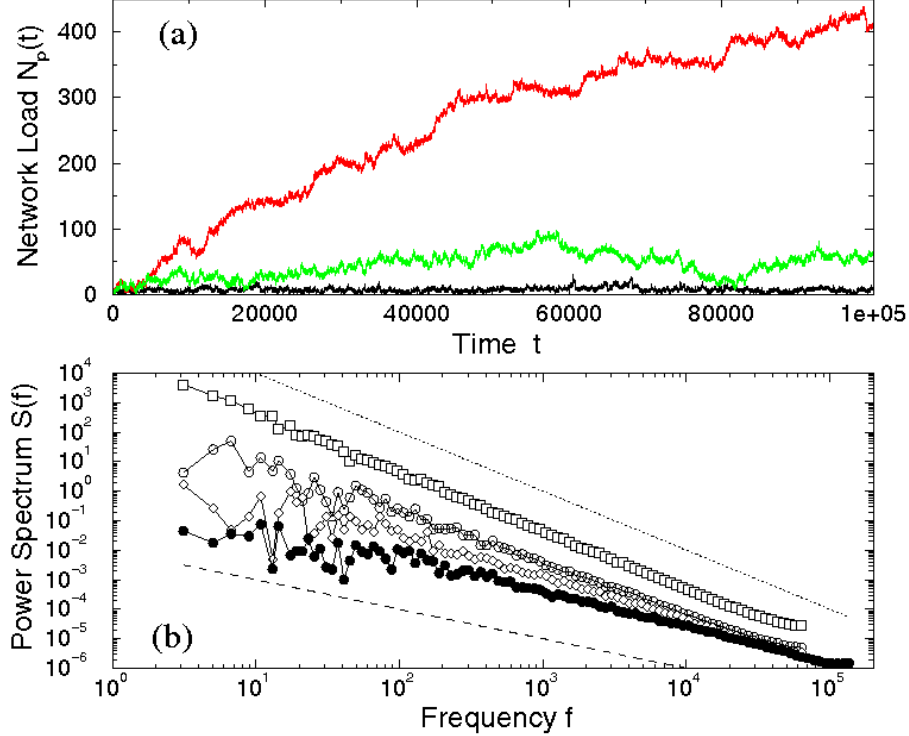


FIG. 11: (a) Network-load $N_p(t)$ time-series for transport on the Webgraph with $nnn-$search and three posting rates indicating (bottom to top) free flow, flow with "crisis", and occurrence of jamming. (b) Power-spectra of $N_p(t)$ time-series for several posting rates below jamming threshold. Dashed and dotted lines indicate limiting slopes with $\phi = 1$ and $\phi = 2$, respectively. The jamming transition corresponds to $\phi = 2$.

In Fig. 11(a) we show the time-series of the network load $N_p(t)$ for three representative posting rates $R =0.25$, 0.35, and 0.45 on the Webgraph. Compared to the time-series of the number of active nodes in Fig. 8, here we take into account that each active node has a queue of packets of a length $Q_i(t) \geq 1$, which contributes to the overall network load, $N_p(t) = \sum_i^N Q_i(t)$. Two of the time-series in Fig. 11(a) are stationary, however, the average load is increasing with the posting rate $R$. Another qualitative difference is that, for the larger posting rate, $R = 0.35$ in this case, a temporary jamming may occur that lasts for approximately 60000 time steps, and eventually resolved by the system itself. This 'crisis'-like behavior is one of the manifestations of the approach to a congested flow regime at a critical posting rate $R_c$. A systematic analysis of the traffic on Statnet for different posting rates $R$ reveals that the average load $< N_p(t) >$ is much larger, compared to the Webgraph, but also that the critical rate where the jamming occurs is twice the critical rate of the Webgraph (see below). In Fig. 12 network-load time-series are shown for two representative posting rates just below the respective jamming point in both networks.

As shown in Ref. [4], on approaching the jamming point, numerous manifestations of developing congestion can be measured statistically. In particular, increased waiting times of packets and characteristic changes in the distribution of waiting times and network loads are detected, as well as in the correlations of the activity and load time-series. For the purpose of this work, we discuss only the systematic changes in the network-load time-series. The power-spectra of the network-load time-series for the traffic on Webgraph are shown in Fig. 11(b) for different values of the posting rate in the range $R = 0.005$ to $R = 0.4$. The remarkable feature of the spectra is the systematic decrease in the correlations (antipersistency), measured by the increased scaling exponnet $\phi$ in Eq. (9) from $\phi = 1.18$ at lowest considered posting rate, to $\phi = 2$, at the jamming threshold. This gives the numerical evidence that the onset of congested state is characterized by a loss of long-range correlations in packet streams. This feature seems to apply generally. The transition to the congested state and the properties of the traffic in the congested regime, however, depend on the topological details of the network.

In order to avoid possible confusion regarding the role of the transition point to the congested state, here we would
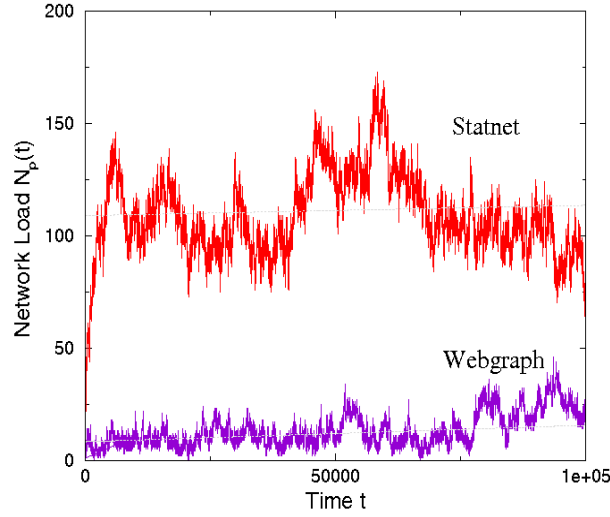
FIG. 12: Network-load time-series close to jamming transitions in Webgraph and Statnet.

like to stress that the network-load time series in our model exhibits long-rage correlations (with an exponent $\phi < 2$) in *a wide range of posting rates below the jamming transition*. As we show in the next subsection, these correlations are strictly related to the structural complexity of the network.

### 3.2. Transition to Congested Traffic State

Technically, the transition point can be identified with $\phi(R_c) \to 2$ for a given network geometry. A characteristic slow-down of the dynamics at a congested node, typically a hub in the Webgraph, occurs in that only one packet can move-in from one of the neighbour nodes, and a large number of packets at other neighbouring nodes are waiting until one packet moves-out the hub in the next time step. Study of long time-series for different posting rates reveals how the de-correlation occurs on different network structures. In Fig. 13 we show values of the exponent $\phi$ against $R$ in the case of Webgraph and Statnet. It shows first that large variations in the strength of correlation occur in load time-series on the Webgraph, in contrast to the time-series on the Statnet, which exhibit weaker but stable correlations over a wider range of posting rates. The values of the critical rates are $R_c \approx 0.4$ for traffic on the Webgraph, whereas $R_c \approx 0.8$ for the Statnet, roughly coincide with the time-series decorrelation rates.

Additional quantitative characteristics of the transition to the congested state can be obtained by measuring the average jamming rate, $J$, which is defined in Eq. (13). In Fig. 13 we show systematic dependences of the jamming rate $J$ from the externally imposed posting rate $R$ for traffic on both types of networks. It reveals that the critical posting rates $R_c = 0.4375 \pm 0.0125$ for traffic on the Webgraph, and $R_c = 0.75 \pm 0.0125$ in the case of Statnet, at which the jamming transition starts to appear are closely associated with a complete decorrelation in the respective time-series ($\phi$ reaches the value of 2 in both cases). Apart from the differences in values of the critical rates $R_c$, the onset of jamming seems to occur abruptly in both networks. Additional differences due to network topology are seen in the character of the jammed traffic. Namely, the slopes of the curves for $J(R)$ above the jamming point in each case are different. This suggests that in the congested state the delivery rate $\lambda$, according to Eq. (13) drops to $\lambda/R = 1 - J/R$, where $J/R = 0.7$ for the case of Webgraph, and $J/R = 0.5$ for the case of Statnet, are slopes of the curves $J(R)$ in Fig. 13. Therefore, in the congested state the Webgraph continues to process about 30% of posted packets, whereas the Statnet manages to deliver about 50%.

At this point it is interesting to compare the constant density traffic, $\rho = 100$ studied in previous section, with the picture of jamming on the two topologies. In the constant density traffic an effective posting rate $< R >$ emerges, which keeps the balance of the network's output rate. According to Fig. 10, for $\rho = 100$ the effective posting rates, $< R >= \lambda = 0.37$ for the Webgraph, and $< R >= \lambda = 0.71$ in the case of Statnet, are below the respective jamming point in both topologies.
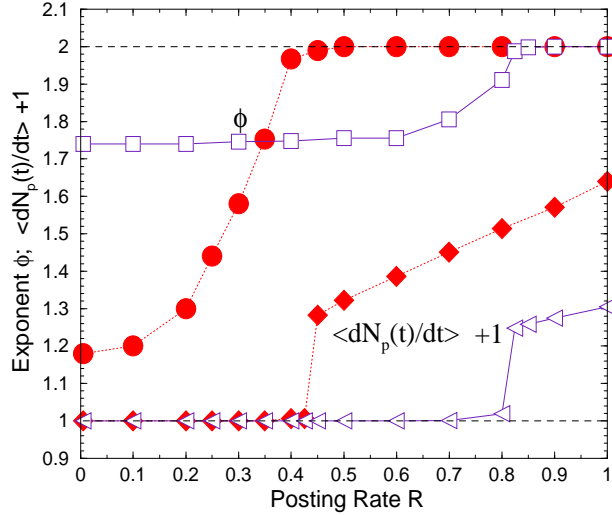
FIG. 13: (upper curves) Correlation exponent $\phi$ defined in Eq. (9) and (lower curves) jamming rate $< dN_p(t)/dt >$ (shifted by 1) for different values of posting rates $R$ in traffic on the Webgraph (filled symbols) and Statnet (open symbols).

## 4. OPTIMIZED TRANSPORT

Perhaps the most important question in transport optimisation is to identify the optimal performance of a network, once certain constraints such as search mode and queue protocols are specified. Here we review two ideas that address this question from different standpoints. The first develops a method to identify optimal paths in different networks by using maximum flow trees [46], the other actually optimises network structure for a given protocol and search depth [28].

### 4.1. Optimal Paths on Fixed Topologies

By simulating a large number of packets we record the number of walks along each link (dynamic flow) and through each node (dynamic noise) in the network. Obviously, the inhomogeneity of nodes with respect to their local network environment, as shown in Fig. 2, makes the flow and noise fluctuations different on each network structure. To obtain a quantitative analysis of flow on the network links, here we construct a *maximum-flow spanning tree*, on which each node is connected to the rest of the network nodes via its maximum-flow link. Implementing a greedy algorithm, we determine the trees from maximum-flow in the $\rho = 1$ limit on the two networks. The trees are shown in Fig. 14.

The structure of these trees reflects both the underlying network geometry and how that geometry effects transport with given navigation rules–local *nnn*-search. In the case of the Webgraph the tree exhibits a scale-free topology, suggesting a certain degree of compatibility between the traffic and the structure. Similarly, for the Statnet the tree shows some degree of inhomogeneity that corresponds to the weaker inhomogeneity of the underlying graph.

The maximum-flow spanning trees represent the union of maximum-flow paths on the underlying network structure. In Fig. 15 we show distribution of the lengths of all such paths on the two trees that are shown in Fig. 14. Once again, differences in the graph topologies and thus in their maximum traffic trees manifest themselves in the statistics of the maximum-flow paths. For instance, the average distance along such paths on the Webgraph and Statnet differs by a factor of about 5, the maximum distance differs by a factor of about 3.

The message is that for a fixed navigation protocol the underlying network structure determines the topology of *optimal paths* for packet transport. These paths consist of links that appeared to be *locally optimal* choices for packets, without any global feedback. The quantitative differences in these topologies can be determined in the limit of non-interacting packets (as shown in Fig. 14). However, how these optimal paths are used by packets when the traffic density is increased, again depends on the properties of the network queues. In particular, the traffic efficiency due to very short paths between pairs of nodes, as on scale-free topologies, can be hindered by the occurrence of large queues at hubs, discussed in Sect. 3. In the following we show what network topologies emerge as *globally optimal structures* in relation to varying traffic density [28].
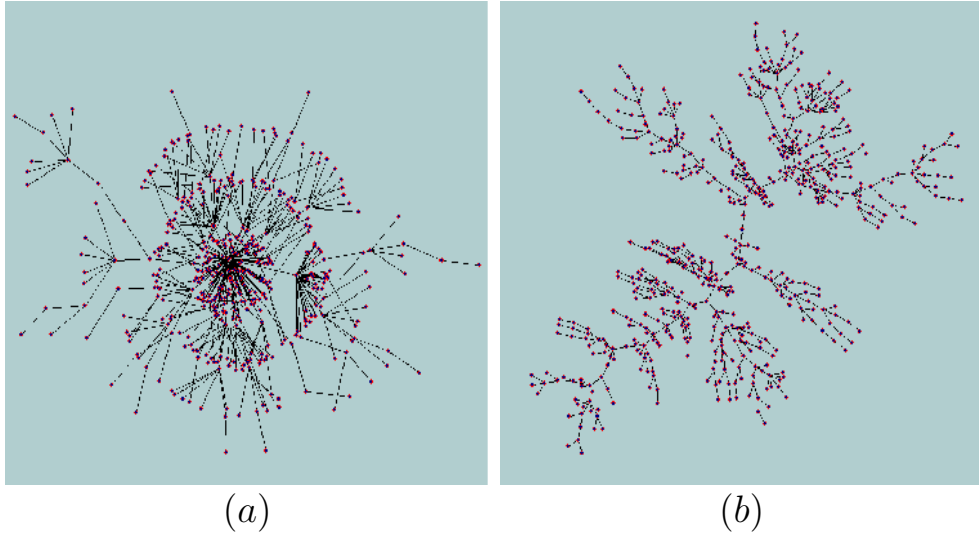
FIG. 14: Dynamic maximum-flow spanning tree traffic density $\rho = 1$ on the cyclic scale-free Webgraph (a) and homogeneous Statnet (b).
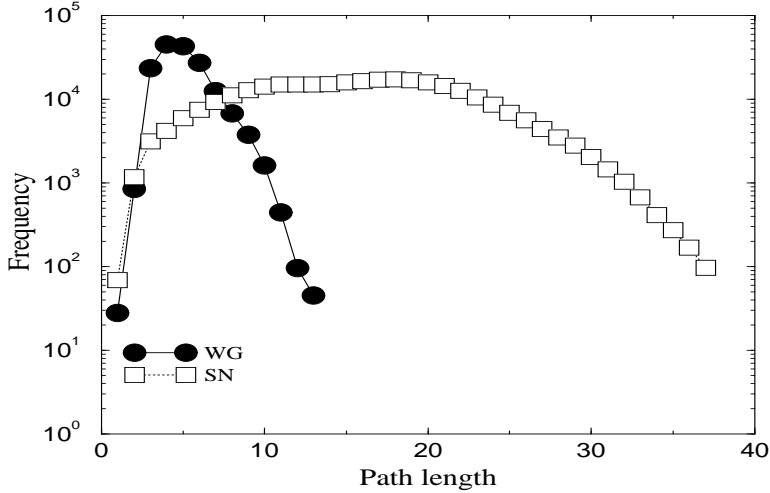


FIG. 15: Distance distributions on the maximum-flow spanning trees for the Webgraph and the Statnet for $\rho = 1$, and $nnn$-search [Tadic and Thurner, 2006].

### 4.2. Traffic Optimization by Network Restructuring

In Sects. 2 and 3 we have demonstrated that transport efficiency on a given network topology may crucially depend on the traffic density. Specifically in strongly inhomogeneous networks, such as the Webgraph, the structural characteristics which are advantageous at low traffic density—occurrence of powerful central nodes, may appear as weaknesses at high density traffic. In this subsection we would like to draw attention to a more systematic way to obtain an optimal structure for a given density using network reconstruction. The suitable formalism was introduced in Ref. [28], where global structure optimization is performed starting from data about individual packet flow. In this respect, the formalism simultaneously accounts for both search and congestion aspects of the information flow on networks. The basic arguments are presented below. For more details see the original Ref. [28].

As before the focus is on a single information packet at node $i$ whose destination is node $k$. The probability for the packet to go from $i$ to a new node $j$ in its next movement is $p_{ij}^k$. In particular, $p_{kj}^k = 0$, $\forall j$ so that the packet is removed as soon as it arrives at its destination. The probability $p_{ij}^k$ depends on the network topology, given by the elements of the adjacency matrix $c_{ij}$, and on the search algorithm. The three cases with local search modify the
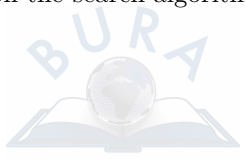
transition probability $p_{ij}^k$ in the following way: For a random walk (searched depth zero) we have

$$p_{ij}^k = \frac{c_{ij}}{\sum_j c_{ij}} \quad , \tag{14}$$

and for a random walk with nearest neighbour search

$$p_{ij}^k = c_{ik}\delta_{jk} + (1 - c_{ik})\frac{c_{ij}}{\sum_j c_{ij}} \quad . \tag{15}$$

Finally, for the the $nnn$-search used in Sects. 2 and 3, it corresponds to

$$p_{ij}^k = \begin{cases} \delta_{jk} & \text{if } c_{ik} = 1 \\ \frac{c_{ij}c_{jk}}{\sum_j c_{ij}c_{jk}} & \text{if } c_{ik} = 0 \text{ and } \sum_j c_{ij}c_{jk} > 0 \\ \frac{c_{ij}}{\sum_j c_{ij}} & \text{if } c_{ik} = 0 \text{ and } \sum_j c_{ij}c_{jk} = 0 \end{cases} \tag{16}$$

Following the Ref. [28], one can then determine the dynamic betweenness of nodes and, subsequently, the network load $N_p(t)$, under certain fairly general conditions. When the search is Markovian, i.e. $p_{ij}^k$ does not depend on previous positions of the packet, the probability of going from $i$ to $j$ in $n$ steps is given by

$$P_{ij}^k(n) = \sum_{l_1, l_2, \ldots, l_{n-1}} p_{il_1}^k p_{l_1 l_2}^k \cdots p_{l_{n-1}j}^k \quad . \tag{17}$$

This definition allows calculation of the average number of times, $b_{ij}^k$, that a packet generated at $i$ and with destination at $k$ passes through $j$. This can be expressed in matrix notation as

$$b^k = \sum_{n=1}^{\infty} P^k(n) = \sum_{n=1}^{\infty} \left(p^k\right)^n = (I - p^k)^{-1}p^k \quad , \tag{18}$$

where the matrices $b^k$, $P^k(n)$ and $p^k$ have elements $b_{ij}^k$, $P_{ij}^k(n)$ and $p_{ij}^k$ respectively and $I$ is the identity matrix. The effective (dynamic) betweenness, $B_j$, of node $j$ is then defined as the sum over all possible origins and destinations of the packets on the graph,

$$B_j = \sum_{i,k} b_{ij}^k \quad . \tag{19}$$

When the search algorithm is able to find the minimum paths between the origin and destination nodes, the *effective* betweenness will coincide with the *topological* betweenness [39, 40, 41], considered in Sec. 2.

If packets are generated at random and independently with a probability $R$, or at each node with probability $r = R/N$, and if the queuing discipline is given by a random queue M/M/1, rather than the more complicated LIFO used in Section 2, it can be shown that the time averaged load of the network is [28, 50]

$$\overline{N_p} = \sum_{j=1}^{N} \frac{\frac{rB_j}{N-1}}{1 - \frac{rB_j}{N-1}} \quad . \tag{20}$$

This solution has two interesting limiting cases: For small values of $r$ the average load is be proportional to the average effective distance [28]. On the other hand, when $r$ approaches a critical rate $r_c$, most of the load of the network comes from the most congested node, and therefore

$$\overline{N_p} \approx \frac{1}{1 - \frac{rB^*}{N-1}} \quad ; \qquad r \to r_c \quad , \tag{21}$$

where $B^*$ is the effective betweenness of the most central node, and assuming that the jump probabilities $p_{ij}^k$ do not depend on the congestion state of the network.

Equation (20) relates a dynamical variable, the load, with topological properties of the network and of the search algorithm. Hence, the dynamical optimization procedure of finding the structure that gives the minimum load is reduced to a topological optimization procedure where the network structure is characterized by its effective (dynamic) betweenness distribution. In [28] the problem of finding optimal structures was considered for a purely local search, Eq. (14), using a generalized simulated annealing procedure, as described in [51, 52]. Surprisingly, it was found that
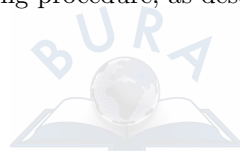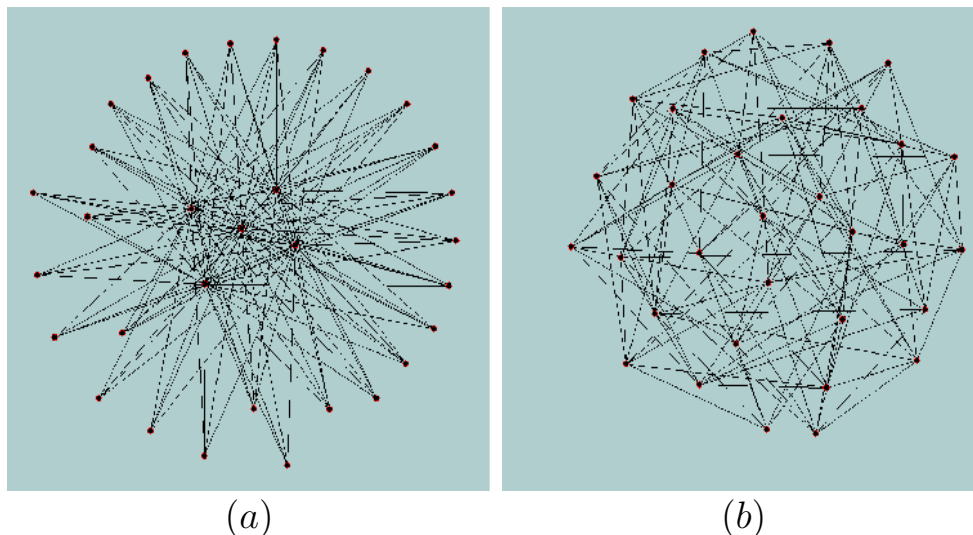
FIG. 16: Optimal networks for low-density traffic (a) and for high-density traffic (b). (Data: courtesy A. Díaz-Guilera.)

there are only two types of structures that can be optimal for a local search process: star-like networks for posting rates below a characteristic rate $R^*$, $r < r^*$ and homogeneous networks for $r > r^*$. The networks are shown in Fig. 16.

The network structures which result from the optimization process for two limits of the traffic density, Fig. 16, exhibit a remarkable similarity with graphs considered in Sec. 2, in particular, with their *core-graphs* (graphs without single-link nodes). This comparison helps us to identify the main topological property of the graphs in Fig. 1 that is responsible for the transport efficiency. In particular, it suggests that the large clustering in the Webgraph near the main hubs is responsible for the increased efficiency of transport at low traffic density [3, 4] (see also Section 3) compared to other scale-free networks. Similarly, the absence of clustering and a narrow distribution of the connectivity in the Statnet, makes it suitable to support a large-density traffic, in analogy to the homogeneous network in Fig. 16.

## 5. OPEN PROBLEMS AND CONCLUSIONS

### 5.1. Summary

We have shown using two complementary approaches that two different classes of network structure give rise to different traffic properties. The classes of network structures we considered were scale free graphs with a significant hub node and high clustering (called Webgraph), and a much more homogeneous network with a quickly decaying degree distribution (called Statnet). These classes were identified in two ways. Firstly, by directly implementing a fairly realistic protocol for packet transport on these networks we demonstrated with a number of quantitative characteristics that the traffic behaves differently on the two networks. Secondly, making use of the results of network optimization in [28], we concluded that these two network classes appear to be representative of optimal structures for low and high traffic density, respectively.

A comparative study of packet transport on these two networks revealed how traffic properties depend on the network structure and on the packet density. We considered both free moving and congested traffic, and driving conditions with both a constant packet density and with a constant posting rate. A summary of the traffic characteristics identified is given below:

*Power-law tails:* In the statistics of individual packets the distributions of travel time, $P(T)$, and waiting time, $P(t_w)$, exhibit power-law tails on both network types, however, with different slopes (cf. Figs. 4, 7). Further differences appear at short travel times, where transport on the Webgraph mostly follows the shortest path between source and destination nodes, while the times up to a characteristic time $T_0 \approx 10$ steps are all equally probable on Statnet. Consequently, the distribution $P(T)$ fits a $q-$exponential [53] in the homogeneous Statnet and a true power-law in the scale-free Webgraph. The distributions of return-time, $P(T_r)$, has power-law tails with a large slope on both networks. The main differences between the networks appear at short return times (see Fig. 5), where the inhomogeneous betweenness of nodes in the Webgraph play an important role.

*Universal noise fluctuations:* The traffic noise averaged over a suitably chosen time window follows the universal law in Eq. (10) in both network classes. In the free flow regime we find $\mu = 1/2$ law in both network types, regardless of the differences in their homogeneity and clustering characteristics. However, when the traffic jamming occurs at large density, the law changes towards $\mu = 1$, for the busiest hub nodes in the inhomogeneous scale-free Webgraph, whereas no qualitative changes are observed in the homogeneous Statnet.

*Antipersistent time-series:* The network load time-series $N_p(t)$ in both network types are found to be antipersistent in the free flow regime. The degree of correlations, however, are considerably different (Fig. 13), depending on traffic density (or posting rate). The noise correlations on Webgraph vary from very strong, at low density, to weak correlations, at the jamming threshold $R_c \approx 0.4$. In the case of homogeneous Statnet the noise correlations are generally weaker but stable in a wide range of posting rates until the jamming threshold, $R_c \approx 0.8$, when only short-range correlations survive.

*Jamming transition:* A jammed traffic regime, characterized by unbalanced increase of network load occurs on both networks at their critical posting rates $R_c$, mentioned above, Fig. 13. The appearance of the nonzero jamming rate $\lambda$ (Eq. 11) is quite sudden for finite sized networks of both classes. For a given network type the value of the critical threshold $R_c$ depends strongly on the efficiency of the search algorithm [3]. Specifically, the critical rate $R_c \approx 0.4$ in traffic with *nnn*-search on the Webgraph is particularly high compared to random diffusion on the same graph or traffic on scale-free trees, where the critical jamming rate is of the order $R_c \approx 10^{-3}$ [3].

*Traffic in the congested state:* The advantage of the homogeneous structure at high traffic density continues to be seen in the congested regime. However, the difference in the efficiency is only about 20%. This can again be attributed to the efficient *nnn*-search of the Webgraph geometry.

*Optimal flow paths:* The union of the optimal paths learnt from the traffic history, summarized at the maximum-flow spanning trees of the two network types in Fig. 14 shows the advantage of the scale-free structure at low density traffic. Due to the efficient search, the maximum-flow tree retains the scale-free character and the statistics of the optimal path lengths in Fig. 15 resemble those of the topologically shortest paths on the graph. On the other hand, paths are much longer on the homogeneous Statnet, independent of the traffic density.

For a fixed network geometry further, although limited, optimization may be achieved by improving the search algorithms [54]. Transport processes on other types of networks, cellular networks [55], gradient networks [56, 57], river networks [58], or generally trees and directed graphs, are subject of additional constraints that may result in qualitatively different behavior. These networks are not considered in the current work.

## 5.2. A comment regarding 'realistic' protocols

Among various transport networks the Internet is an particularly accessible and attractive example. In recent years measurements in both the Internet structure and the information packet TCP/IP traffic dynamics on the Internet have been carried out and their inter-relations discussed [59, 60, 61, 62, 63, 64]. These have either considered ping time statistics, that is a packet's round trip time from source to destination and back again, or the statistics of the load on a particular server, router or cable. Almost all these studies have found scaling laws and long range correlations in a range of traffic time-series [59, 60, 61]. Examination of the power spectra has allowed the identification of two different regimes with free flow or jammed traffic. It was shown [65] that the power-law behaviour of the distribution of packet inter-arrival times has a significant impact on packet queue statistics, and consequently on the overall traffic performance.

In addition, the scale-free nature of the Internet structure [64, 66] has been fully characterised. The structural characteristics on the autonomous systems level, in particular the degree distribution, high clustering and link-correlations, are statistically similar to those of the prototype network Webgraph discussed in Sec. 2. Beyond the practical importance of research into the properties of the Internet, the underlying cause of self-similarity and criticality in the Internet's structure and information traffic is still a subject of debate involving researchers in a broad range of scientific disciplines. Among the goals of this research is to determine universality classes of the scale-free behaviour and to unravel the mechanisms of the structure–dynamics interdependences.

Examining our results in Sec. 2, obtained with the local *nnn*-navigation algorithm, we can conclude that the statistical features of the traffic, in particular the power-law distributions, the degree of correlations in the packet streams, and the onset of jamming, are related to the actual Internet structure. Furthermore, our results suggest that no substantial improvement in traffic efficiency will be achieved by implementing a long-range search beyond the "critical horizon" of the scale-free network, which is depth level two in our Webgraph (more detailed analysis is given in [43]). In the study by [13], who first introduced the term "critical path horizon" in this context, the sharp transition was found at the depth level four. The difference in the critical horizons in these two scale-free networks can be attributed to the better "searchability" of the correlated scale-free Webgraph, compared to uncorrelated scale-free network used in [13].

Of crucial importance is the centrality of nodes, which pre-determines the size of queues, and hence the traffic jamming and an increased risk of packet loss. The onset of traffic congestion seems to occur suddenly in the prototype network, and is probably related to the size of the giant cluster. However, we observed a kind of traffic "crisis" behaviour with large load fluctuations before the actual jamming starts. The statistical indicators of the traffic behaviour, determined in previous sections, systematically change with the increased network load (traffic density). Hence the following four phases can be clearly identified: Free flow, crisis, jamming threshold and congested traffic. Therefore, an effective control mechanism, that would eventually lead to increased traffic efficiency and security, may be developed through a systematic monitoring of one or more of these indicators.

### 5.3.  Some Open Theoretical Problems in Transport on Networks

Quantitative properties of transport on a network topology depend in different ways on the *network geometry* and on *search algorithm* and *type of queues* on that geometry. The actual dependence on the search and queuing cannot be considered independently of the underlying network structure [43]. Another subtle factor which determines the transport properties is the *driving mode*. Specifically, large fluctuations of the posting rate may influence noise properties. More seriously, they may drive the network out of a stationary flow, where some statistical properties cannot be determined mathematically correctly.

For the theoretical purposes we have implemented in Sec. 2 a non-invasive *self-consistent* driving, which preserves the number $\rho$ of moving packets in time. The stationarity of time-series is thus guaranteed, and jamming does not occur when $\rho$ is not too big, as shown above. In this regime we can determine numerically the correct statistical properties of the traffic. In the limit $\rho \to 1$ the outcomes are directly attributed to the network structure. The results of numerical simulations are given in Sec. 2. However, clear theoretical concepts behind these numerical results still remain elusive, in particular related to the following questions:

- Universality classes of travel time distributions.

- Power-laws in the waiting time distribution.

- Queue interactions in the correlated network environment.

- Return-time distributions structural dependences and occurrence of the $q-$exponential.

- Robustness of the universal noise fluctuations, related to traffic density and network structure.

- Universality of the dynamic jamming transition.

In traffic models, as in many other dynamical systems, power-law behaviour is often attributed to (dynamic) phase transitions, separating different attractors of the dynamics. A particular example of this is the jamming transition in the traffic model on a compact lattice studied by [7]. However, when the underlying network is sparse and strongly inhomogeneous, additional correlations may become relevant, leading to attractive states with self-similar dynamics away from the phase transition. In this paper, by comparing traffic on different networks, we have found substantial evidence that the self-similar dynamic properties (at and away of the jamming transition) are shaped by the network geometry.

In conclusion, the dynamic characteristic of transport processes on networks, appear to be, to a large extent, pre-designed by the underlying network structure, where certain structural characteristics play a dominant role. However, these structure–function interdependences are strongly determined by the dynamic conditions, in particular traffic density. In this respect, two large classes of networks with an optimal function are now identified—clustered scale-free networks, and homogeneous, or weakly structured, unclustered networks. With the large-scale numerical simulations in this work we have shown that different quantitative characteristics of the traffic emerge in these two network classes. This leaves open the question about the active principle which shapes the dynamics within each of these network classes. We hope that our investigations will initiate further theoretical and practical research to address this question.

P10 Physics of Risk, is acknowledged.

———————————

[1] S. Boccaletti, V. Latora, Y. Moreno, M. Chavez, and D.-U. Hwang, Phys. Rep. **424**, 175 (2006).
[2] B. Tadić and G. Rodgers, Advances in Complex Systems **5**, 445 (2002).
[3] B. Tadić and S. Thurner, Physica A **332**, 566 (2004).
[4] B. Tadić, S. Thurner, and G. J. Rodgers, Phys. Rev. E **69**, 036102 (2004).
[5] A. Arenas, A. Díaz-Guilera, and R. Guimerà, Phys. Rev. Lett. **86**, 3196 (2001).
[6] R. Guimerà, A. Arenas, A. Díaz-Guilera, and F. Giralt, Phys. Rev. E **66**, 026704 (2002).
[7] R. V. Sole and S. Valverde, Physica A **289**, 595 (2001).
[8] S. Valverde and R. V. Solé, Physica A **312**, 636 (2002).
[9] T. Ohira and R. Sawatari, Phys. Rev. E **58**, 193 (1998).
[10] Y. Moreno, R. Pastor-Satorras, A. Vázquez, and A. Vespignani, Europhysics Letters **62**, 292 (2003).
[11] M. Rosvall, P. Minnhagen, and K. Sneppen, Phys. Rev. E **71**, 066111 (2005).
[12] M. Rosvall and K. Sneppen, Phys. Rev. Lett. **91**, 178701 (2003).
[13] S. Valverde and R. V. Sole, Eur. Phys. J. B **38**, 245 (2004).
[14] W.-X. Wang, B.-H. Wang, C.-Y. Yin, Y.-B. Xie, and T.Zhou, Rhys. Rev. E **73**, 026111 (2006).
[15] H. Agrawal, Phys. Rev. Lett. **89**, 268702 (2002).
[16] S. Thurner, R. Hanel, and S. Pichler, Quantitative Finance **3**, 306 (2003).
[17] M. Boss, H. Elsinger, M. Summer, and S. Thurner, Quantitative Finance **4**, 677 (2004).
[18] R. Coelho, Z. Neda, J. Ramasco, and M. Santos, Physica A **353**, 515  (2005).
[19] Y. Moreno, M. Nekovee, and A. F. Pacheco, Phys. Rev. E **69**, 066130 (2004).
[20] M. E. J. Newman, Phys. Rev. E **66**, 016128 (2002).
[21] M. Boguñá, R. Pastor-Satorras, and A. Vespignani, in *Statistical Mechanics of Complex Networks*, edited by R. Pastor-Satorras, M. Rubi, and A. Díaz-Guilera (Springer Verlag, Berlin, 2003), vol. 625 of *Lecture Notes in Physics*.
[22] B. Tadić, European Physical Journal B **23**, 221 (2001).
[23] J. D. Noh and H. Rieger, Phys. Rev. Lett. **92**, 118701 (2004).
[24] Z. Eisler and J. Kertesz, Phys. Rev. E **71**, 057104 (2005).
[25] L. K. Gallos, Phys. Rev. E **70**, 046116 (2004).
[26] V. Latora and M. Marchiori, Phys. Rev. Lett. **87**, 198701 (2001).
[27] T. C. Jarrett, D. J. Ashton, M. Fricker, and N. F. Johnson, ArXiv Physics e-prints (2005), arXiv:physics/0508228.
[28] R. Guimerà, A. Díaz-Guilera, F. Vega-Redondo, A. Cabrales, and A. Arenas, Phys. Rev. Lett. **89**, 248701 (2002).
[29] P. Holme, Advances in Complex Systems **6**, 163 (2003).
[30] P. Echenique, J. Gomez-Gardenes, and Y. Moreno, Europhysics Letters **71**, 325 (2005).
[31] D. J. Ashton, T. C. Jarrett, and N. F. Johnson, Phys. Rev. Lett. **94**, 058701 (2005).
[32] Z. Burda, J. Jurkiewicz, and A. Krzywicki, Phys. Rev. E **70**, 026106 (2004).
[33] S. N. Dorogovtsev and J. F. Mendes, *Evolution of Networks: From Biology to the Internet and WWW* (Oxford University Press, 2003).
[34] B. Tadic, Physica A **293**, 273 (2001).
[35] R. Albert and A.-L. Barabasi, Review of Modern Physics **74**, 47 (2002).
[36] B. Tadić, in *Computational Science — ICCS 2003*, edited by P. Sloot *et al.* (Springer, 2003), vol. 2657 of *Lecture Notes in Computer Science*, pp. 136–143.
[37] B. Tadić and V. Priezzhev, European Physical Journal B **30**, 143 (2002).
[38] B. Tadić, Physica A **314**, 278 (2002).
[39] M. Newman, Rhys. Rev. E **64**, 016132 (2001).
[40] T. Zhou, J.-G. Liu, and B.-H. Wang, arXiv:physics/0511084 (2005).
[41] V. Latora and M. Marchiori, cond-mat/0402050 (2004).
[42] M. E. J. Newman, Phys. Rev. E **67**, 026126 (2003).
[43] B. Tadić and S. Thurner, Physica A **346**, 183 (2005).
[44] A. Arenas, A. Cabrales, A. Díaz-Guilera, R. Guimerà, and F. Vega-Redondo, in *Proceedings of the Conference Statistical Mechanics of Complex Networks*, edited by R. Pastor-Satorras, M. Rubi, and A. Díaz-Guilera (Springer Verlag, Berlin, 2003), vol. 625 of *Lecture Notes in Physics*.
[45] W. Whitt, *Stochastic-Process Limits* (Springer, New York, 2001).
[46] B. Tadić and S. Thurner, in *ICCS 2006*, edited by V. Alexandrov*et al.* (Springer, Berlin, 2006), vol. 3993 of *Lecture Notes in Computer Science*, pp. 1016–1023.
[47] M. Argollo de Menezes and A.-L. Barabási, Phys. Rev. Lett. **92**, 028701 (2004).
[48] J. Duch and A. Arenas, physics/0602077 (2006).
[49] Z. Eisler and J. Kertesz, Phys. Rev. E **73**, 046109 (2006).
[50] O. Allen, *Probability, statistics and queueing theory with computer science application* (Academic Press, New York, 1990).
[51] C. Tsallis and D. A. Stariolo, in *Annual Review of Computational Physics II*, edited by D. Stauffer (World Scientific, Singapore, 1994).

[52] T. Penna, Phys. Rev. E **51**, R1 (1995).

[53] C. Tsallis, J. Stat. Phys. **52**, 479 (1988).

[54] B. Kujawski, G. Rodgers, and B. Tadić, in *ICCS 2006*, edited by V. Alexnandrov *et al.* (Springer, Berlin, 2006), vol. 3993 of *Lecture Notes in Computer Science*, pp. 1024–1031.

[55] M. Šuvakov and B. Tadić, Physica A p. ?? (2006).

[56] Z. Toroczkai and K. Bassler, Nature **428**, 716 (2004).

[57] K. Park and Y.-C. Lai, Phys. Rev. E **71**, 065105 (2005).

[58] J. Banavar, A. Maritan, and A. Rinaldo, Nature **399**, 130 (1999).

[59] I. Csabai, Journal of Physics A Mathematical General **27**, L417 (1994).

[60] M. Takayasu, H. Takayasu, and T. Sato, Physica A **233**, 824 (1996).

[61] M. Takayasu, H. Takayasu, and K. Fukuda, Physica A **277**, 248 (2000).

[62] W. Willinger, R. Govindan, S. Jamin, V. Rexons, and S. Shenker, PNAS **99**, 2573 (2002).

[63] S. Abe and N. Suzuki, Europhys. Lett. **61**, 852 (2003).

[64] D. Doyle, D. Alderson, L. Li, S. Low, M. Roughan, S. Shalunov, R. Tanaka, and W. Willinger, PNAS **102**, 14497 (2005).

[65] W. Willinger, M. Taqqu, R. Sherman, and D. Wilson, IEEE/ACM Trans. Networking **5**, 711 (1997).

[66] A. Vázquez, R. Pastor-Satorras, and A. Vespignani, Phys. Rev. E **65**, 066130 (2002).